Viscous-Inviscid Interaction

Veldman, Arthur E.P.

Link to publication in University of Groningen/UMCG research database

Viscous-Inviscid Interaction:
Prandtl's Boundary Layer challenged by Goldstein's Singularity

Arthur E. P. Veldman

Institute of Mathematics and Computing Science, University of Groningen
P.O. Box 800, 9700AV Groningen, The Netherlands
veldman@math.rug.nl

1. Prandtl's boundary layer

Almost exactly 100 years ago the history of the development of viscous-inviscid interaction methods began. To be precise, it began in Heidelberg at 11:30 a.m. on August 12, 1904, when Ludwig Prandtl presented the 'boundary layer' before an audience of mathematicians attending the Third International Mathematical Congress [57] (see also [56]). For decades, scientists had been confused by d'Alembert's Paradox ('discovered' in 1752), stating that *"there is no drag on a finite body at rest in an infinite, incompressible, inviscid flow otherwise in uniform motion"* [70]. Prandtl described how the hardly visible boundary layer near the surface of the body resolves this paradox through the influence of viscosity.
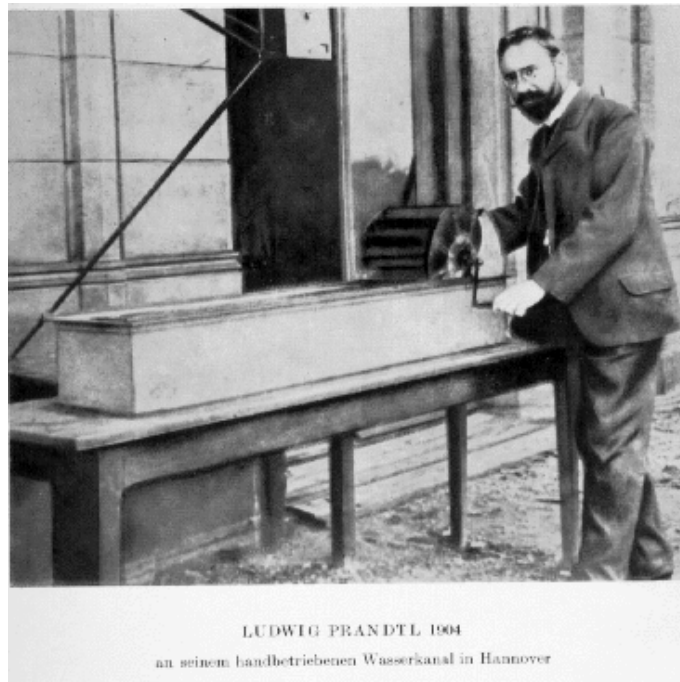
Figure 1: Ludwig Prandtl (1875-1953) experimenting with his manually operated water tunnel in Hannover (1904) [24].

Prandtl's Heidelberg lecture is a landmark in the development of a branch of mathematics nowadays called 'matched asymptotic expansions', although various roots of the boundary-layer idea can be found already in the 19th century [74]. The method of matched asymptotic expansions treats differential equations where a small parameter multiplies the highest derivative, i.e. setting the small parameter at zero implies dropping one (or more) boundary conditions. As a consequence, a series development in the small parameter is no longer valid uniformly
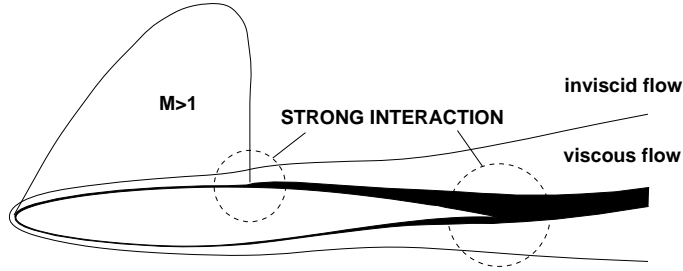
Figure 2: Subdivision of the flow field around an airfoil in an inviscid-flow region and a viscous shear layer (exaggerated in thickness).

throughout the domain. Next to the boundary where in the small-parameter limit boundary conditions have to be dropped, a thin layer has to be added where a different series development is required. Prandtl named this thin layer *Grenzschicht* (English translation: boundary layer), a name that has been used ever since for similar thin layers in other applications.

In aerodynamic applications (Fig. 2), the boundary layer is driven by the inviscid pressure distribution p_e and (through Bernoulli's law) its related streamwise velocity u_e. In the boundary layer the streamwise velocity component is reduced to zero in order to comply with the no-slip condition at the surface. The lateral coordinate y, together with its corresponding velocity component v, scales with the inverse square root of the Reynolds number Re (defined in the usual way[1]). The flow equations can be simplified by neglecting the viscous streamwise derivatives, whereas the lateral momentum equation states the pressure to be constant through the boundary layer. Prandtl's *Grenzschichtgleichungen* emerge (in non-dimensional form):

$$\frac{\partial u}{\partial x} + \frac{\partial v}{\partial y} = 0 \ , \quad u\frac{\partial u}{\partial x} + v\frac{\partial u}{\partial y} = u_e\frac{\mathrm{d}u_e}{\mathrm{d}x} + \frac{1}{\mathrm{Re}}\frac{\partial^2 u}{\partial y^2} \ , \tag{1}$$

with boundary conditions

$$u(x,0) = v(x,0) = 0 \ ; \quad u(x,y_e) = u_e(x) \ ,$$

where y_e denotes the outer edge of the boundary layer.

Effectively, the boundary layer changes (thickens and smoothes) the shape of the geometry. The resulting effective shape is called the displacement body $y = \delta^*$; it becomes a streamline for the inviscid flow (e.g. Lighthill [43]).

The main advantage of the boundary-layer concept is that the elliptic character of the Navier–Stokes equations is changed into a much easier handled parabolic character. The latter was very relevant in an era where mainly analytical tools were available for solving differential equations. The stable direction of the boundary-layer equations (1) is governed by the sign of u. Hence this direction switches in reversed-flow regions, which has implications for the way they are solved, as we will see below.

2. Goldstein's singularity

For situations with attached flow the boundary layer provides only a small perturbation to the inviscid flow. However, it is found that as soon as the flow wants to separate from the body surface, the steady boundary-layer calculation breaks down with a solution that tends to become singular. In his now famous paper of 1948, Goldstein [23] describes the computational findings of his colleague Hartree as follows: *"All computations in which any attempt was made to obtain*

---

[1]All variables have been made dimensionless with a characteristic length scale L and a characteristic velocity scale U. Re$= UL/\nu$, where ν is the kinematic viscosity.

real accuracy at and near separation seem to have met with considerable difficulty. As a result of his computations, Professor Hartree was convinced that there was a singularity in the solution at the point of separation." A number of possible causes for the computational problems can easily be imagined:

i) The growth of the solution violates the assumption made in boundary-layer theory that streamwise derivatives are small. The remedy would be to include these streamwise derivatives in the equations of motion, but then the elliptic character of the Navier–Stokes equations is retained with its corresponding much higher computational complexity.

ii) The stable parabolic direction of the boundary-layer equations changes locally in reversed-flow regions, with negative streamwise velocity. As a consequence, in these regions the equations should be solved from downstream to upstream, hence one single downstream-marching computational sweep does not suffice anymore.

Now, one has to keep in mind that in the first half of the century there were hardly any appropriate tools to solve the flow equations. At that time it was impossible to check the above two possibilities, and the issue had to remain open.

Inspired by the mathematical and numerical challenge, Goldstein [23, p. 45] *"undertook to try to find some formulae that would hold near this singularity and would help in finishing the computation."* As a result, he presented an in-depth discussion on the breakdown of the boundary-layer equations at separation in which he added some more possible causes. Since then, the singularity at separation bears his name. In particular, on page 50 of his paper, Goldstein formulates the following suggestion: *"Another possibility is that a singularity will always occur except for certain special pressure variations in the neighbourhood of separation, and that, experimentally, whatever we may do, the pressure variations near separation will always be such that no singularity will occur."*

It took twenty more years before algorithms and computers were sufficiently developed to perform some numerical experiments in order to explore the options mentioned above. One of these experiments was described in 1966 by Catherall and Mangler [6], who tried to solve the steady boundary-layer equations with prescribed displacement thickness. Indeed, they succeeded to pass the point of flow separation, but ran into difficulties a bit further downstream. The reason hereof is clear, and in fact was already formulated by the authors [6, p. 178]: *"This is possibly to be expected, since the region of reversal flow should really be integrated in the negative ξ-direction with boundary conditions provided from downstream."* With current computer power, this problem is easily remedied by a downstream discretization of the convective terms and subsequent repeated sweeps through the boundary layer. Nevertheless, as Catherall and Mangler were not convinced of their success, they stopped further research into this subject. In fact, Catherall learned only some twenty years after publication about the large impact their paper had created [private communication, 1992].

3. The asymptotic nature of viscous-inviscid interaction

3..1. Hierarchy

In the late sixties, inspired by ideas put forward by Lighthill in 1953 [42], Stewartson (for steady subsonic and supersonic flow) [68, 72], Messiter (subsonic) [48] and Neiland (supersonic) [52] developed asymptotic theories in the neighbourhood of singular points in the flow field, such as a trailing edge or a point of flow separation.

In broad, qualitative lines their reasoning is as follows. Let us start in a hierarchical way with a given pressure distribution (usually obtained from the inviscid-flow equations) to which the boundary layer is assumed to give a (minor) correction. Near a point of flow separation, or another singular point, it is anticipated that the relevant physical length scale in streamwise

direction becomes smaller. As a result the x-derivative in the continuity equation in (1) becomes larger, and consequently so does the vertical velocity component. This translates into a more sudden displacement effect acting upon the external inviscid flow, and with Bernoulli's law it results in a larger pressure disturbance. As soon as this disturbance becomes of the same order as the initially applied pressure distribution the assumption of hierarchy becomes violated. Both inviscid flow and boundary layer now have an equal say in the resulting pressure distribution. In aerodynamical terms, the hierarchy between boundary layer and inviscid flow changes from *weak* interaction into *strong* interaction.

Lagerstrom [38, p. 209] in 1975 described the situation as follows: *"An important feature is that the pressure is self-induced, that is, the pressure due to displacement thickness is determined simultaneously with the revised boundary layer solution. [...] this solution exhibits a definite loss of hierarchy."* This lack of hierarchy should also be visible in the numerical information exchange between boundary layer and inviscid flow, thus guiding their appropriate numerical iterative treatment; see Section 5..

For supersonic flow, a similar conclusion about the boundary-layer interaction near a point of flow separation was reached already sixteen years earlier, as described by Hayes and Probstein in their monograph on hypersonic flow [26, p. 365]: *" ... in general it requires solving simultaneously the integrated momentum and energy equations and the inviscid flow relation describing the pressure along the curve $y = \delta^*(x)$."* One should realise, of course, that here the inviscid flow is supersonic and the interaction (by a local Prandtl–Meyer relation) is of hyperbolic instead of elliptic nature (see below).

3..2. The triple deck

To reach the insight behind the above paragraphs, it took a great intellectual effort of the above-mentioned authors. And because of the impact of their work, in this section we will give a more quantitative asymptotic description of the flow near singular points.

Thus, let us consider a narrow region around a singular point S, of extent

$$x - x_S = O(\mathrm{Re}^{-\alpha}) \,, \quad 0 < \alpha < \tfrac{1}{2} \,, \quad \text{with a scaled coordinate } x_\alpha = (x - x_S)\mathrm{Re}^\alpha \,,$$

where x-derivatives will be more important than assumed thus far. The restriction $\alpha < 1/2$ implies that the width is larger than the boundary-layer thickness, hence x-derivatives remain less important than y-derivatives, which simplifies the analysis. Further it may be anticipated that in vertical direction close to the singular point something happens: say at a y-scale given by $\mathrm{Re}^{-\beta}$ with $\beta > 1/2$ (which is smaller than the boundary-layer thickness).

The oncoming boundary-layer thickness $y = O(\mathrm{Re}^{-1/2})$ will play a role as well. Here the velocity profile immediately before the singular point can be written as ($\tilde{y} = \mathrm{Re}^{1/2}y$)

$$u(x_S, y) = B'(\tilde{y}) + O(\mathrm{Re}^{-1/2}) \,, \quad \text{where for } \tilde{y} \downarrow 0 : \ B(\tilde{y}) \sim \tfrac{1}{2}a\tilde{y}^2 \,. \tag{2}$$

The function $B'(\tilde{y})$ is known, e.g. it is a Blasius profile where $a = 0.332$. Also the y-scale $y = O(\mathrm{Re}^{-\alpha})$ will play a role, since there x-derivatives are as large as y-derivatives.

This three-layered structure, called the triple deck, is sketched in Fig. 3. What is left to find are the particular values for α and β, the modelling pertinent to the individual flow domains, and the flow of information between the separate decks. The latter point turns out to be of crucial importance for the design of numerical solution methods.

To obtain the required insight into the triple-deck behaviour it is unavoidable to go into some detail, therefore we will next give a short resume of the derivation of the (incompressible) triple deck, based on an earlier presentation in [77].
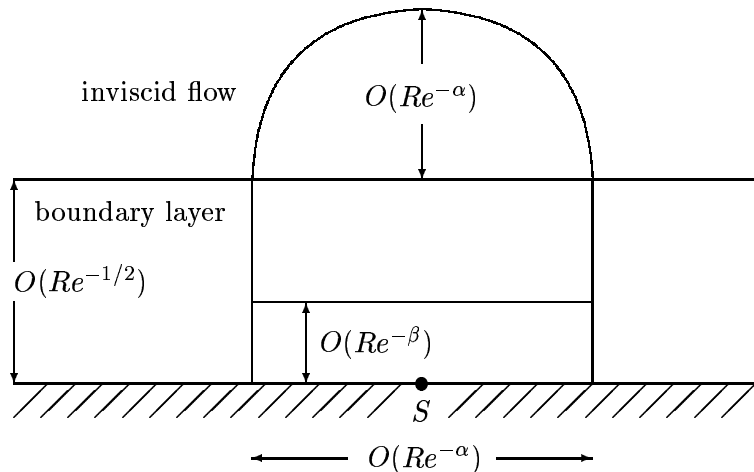
4

Figure 3: The triple deck describes the asymptotic flow structure near singular points.

The lower deck $y = O(\mathrm{Re}^{-\beta})$

In the lower deck the viscous terms balance with the convective terms. For small values of $\tilde{y}$, (2) implies that the oncoming velocity profile is given by $u \sim a\tilde{y}$. Hence, for $y = O(\mathrm{Re}^{-\beta})$ the horizontal velocity is of magnitude $u = O(\mathrm{Re}^{1/2-\beta})$. An estimate of the convective and diffusive terms gives for $x = O(\mathrm{Re}^{-\alpha})$:

$$\text{convection} \quad u\frac{\partial u}{\partial x} = O(\mathrm{Re}^{1-2\beta+\alpha}) \; ; \quad \text{diffusion} \quad \frac{1}{\mathrm{Re}}\frac{\partial^2 u}{\partial y^2} = O(\mathrm{Re}^{\beta-1/2}) \; .$$

Balancing these terms yields a relation between α and β:

$$\beta = \frac{\alpha}{3} + \frac{1}{2} \; .$$

For this value of β the horizontal velocity scales like $u = O(\mathrm{Re}^{-\alpha/3})$, whereas the balancing pressure gradient is $p = O(\mathrm{Re}^{-2\alpha/3})$.

Substitution of these estimates in the Navier–Stokes equations reveals that the flow in the lower deck is still governed by Prandtl's boundary-layer equations, with a pressure that is again constant in vertical direction: $p(x,y) = \mathrm{Re}^{-2\alpha/3}P(x_\alpha)$. High in the lower deck, for $y_\beta = \mathrm{Re}^{\beta}y \to \infty$, we have

$$u(x_\alpha, y_\beta) \sim \mathrm{Re}^{-\alpha/3}\{ay_\beta + aG(x_\alpha) + \cdots\} \; . \tag{3}$$

The function G is related to the displacement thickness, as will be clear in (4) below.

Next to the solid-wall conditions at $y_\beta = 0$, as a first boundary condition at infinity the coefficient of y_β (i.e. a) is given. Additionally, another boundary condition is required. In the classical interpretation this would be the prescription of the pressure, i.e. $P(x_\alpha)$, but in the spirit of Catherall and Mangler [6] this could also be a displacement effect, i.e. $G(x_\alpha)$.

It is stressed that in this way the lower-deck equations form one relation between P and G. A second relation can be found by matching with the other decks, as will be described next.

The middle deck $y = O(\mathrm{Re}^{-1/2})$

In order to concentrate on the essential properties of the triple deck, the derivation of the asymptotic expansions in the middle deck is only summarized. For more details, the reader is referred to the original papers by Stewartson [68] and Messiter [48] (or later papers by e.g. Meyer [49] and Nayfeh [51]).

5

The middle deck is determined through matching with the oncoming flow (2) and the lower deck (3). It 'simply' shows a vertical shift of the oncoming velocity profile, caused by the displacement effect of the lower deck. The expansions in the middle deck are

$$
\begin{aligned}
u(x,y) &\sim B'(\tilde{y}) + \mathrm{Re}^{-\alpha/3} B''(\tilde{y}) G(x_\alpha) + \cdots , \\
v(x,y) &\sim -\mathrm{Re}^{2\alpha/3-1/2} B'(\tilde{y}) G'(x_\alpha) + \cdots .
\end{aligned}
\tag{4}
$$

The leading term in the pressure, once again, turns out to be constant in y-direction $p(x,y) \sim \mathrm{Re}^{-2\alpha/3} P(x_\alpha)$. This information is now passed on to the upper deck.

The upper deck $y = O(\mathrm{Re}^{-\alpha})$

In the upper deck the x- and y-dimensions are equal, whereas viscous effects are not important. It is governed by inviscid flow where Laplace's equation and Bernoulli's law hold.

As $B'(\tilde{y}) \to 1$ for $\tilde{y} \to \infty$, the vertical velocity in (4) induces a velocity $-\mathrm{Re}^{2\alpha/3-1/2} G'(x_\alpha)$ in the upper deck, which according to 'Laplace' leads to a horizontal velocity perturbation

$$
\tilde{u}(x_\alpha, y_\alpha) = -\frac{1}{\pi} \mathrm{Re}^{2\alpha/3-1/2} \int_{-\infty}^{\infty} \frac{G'(\xi)(x_\alpha - \xi)}{(x_\alpha - \xi)^2 + y_\alpha^2} \, \mathrm{d}\xi .
\tag{5}
$$

When in Bernoulli's law $p + (u^2 + v^2)/2 = C$ one substitutes $u = 1 + \tilde{u}$ and $v = \tilde{v}$, with $\tilde{u} \ll 1$ and $\tilde{v} \ll 1$, then to first approximation

$$
p + \tilde{u} = C - 1/2.
\tag{6}
$$

This implies that also the pressure expansion contains a term of order $\mathrm{Re}^{2\alpha/3-1/2}$, which is hence related to displacement effects.

Matching of middle and upper deck now yields two kinds of pressure terms in an expansion that reads

$$
p(x,y) = \mathrm{Re}^{-2\alpha/3} p^{(p)}(x_\alpha, y_\alpha) + \mathrm{Re}^{2\alpha/3-1/2} p^{(\delta)}(x_\alpha, y_\alpha) + \cdots .
\tag{7}
$$

The term $p^{(p)}$ matches the pressure in the middle deck, hence it satisfies $p^{(p)}(x_\alpha, 0) = P(x_\alpha)$; the term $p^{(\delta)}$ is due to displacement effects and through (6) it is related to the horizontal velocity perturbation induced by (5).

Loss of hierarchy

Figure 4 shows the relative order of the two terms present in (7), and herewith it reveals the essential character of the triple deck.

When $\alpha < 3/8$ the term $p^{(p)}$ is the larger one in (7), and it determines, as usual, the pressure P in the boundary layer. The lower-deck equations then provide G after which the second term $p^{(\delta)}$ can be determined, which in turn provides a pressure correction in the boundary layer. The classical hierarchy between inviscid flow and boundary layer is recognized.

This situation changes for $\alpha = 3/8$ when both pressure terms in (7) are equally important, and this is what constitutes the essence of the triple deck. The pressure terms $p^{(p)}$ and $p^{(\delta)}$ have to be identical, thus by equating their values at $y_\alpha = 0$, from (5) and (6) a second relation between P and G is obtained:

$$
P(x_\alpha) = \frac{1}{\pi} \int_{-\infty}^{\infty} \frac{G'(\xi)}{x_\alpha - \xi} \, \mathrm{d}\xi .
\tag{8}
$$

The triple-deck equations now consist of Prandtl's boundary-layer equations, with boundary condition (3) and a second relation between pressure and displacement given by the Cauchy–Hilbert integral (8). The latter is responsible for the elliptic character of the mathematical formulation. The first numerical solutions to the triple-deck equations have been presented in the mid-seventies [33, 46, 82].
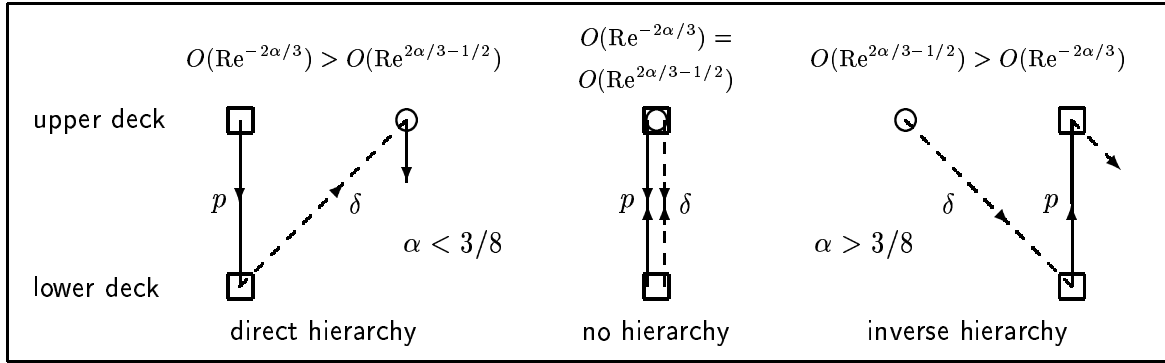
Figure 4: Hierarchy between pressure contributions in lower and upper deck at a streamwise length scale $x = O(\text{Re}^{-\alpha})$.

Remark 1 Parallel to the above subsonic triple deck, a supersonic version was developed by Stewartson and Williams [72]. It is similar, except for the description of the interaction with the inviscid flow. The *global* Cauchy–Hilbert integral (8) is replaced by a *local* Prandtl–Meyer relation

$$P(x_\alpha) = -G'(x_\alpha) .$$

Because of its hyperbolic character the numerical treatment of the supersonic equations is relatively easy: in the absence of reversed flow a single marching sweep through the boundary layer suffices [72].

Remark 2 The triple deck has been the inspiration of a wealth of research on asymptotic descriptions; refer for example to the review papers by Stewartson [69], Smith *et al.* [59, 61, 62, 64] and Kluwick [36], and the monograph by Sychev *et al.* [73].

Remark 3 The above interactive boundary-layer concept is restricted to mildly separated flows, i.e. flows where the thickness of the reversed-flow region is comparable to the boundary-layer thickness. For larger regions of reversed flow (marginal separation or, larger still, massive separation) the asymptotic structure has to be revised [19, 71]. In the same time, the flow in these larger separated-flow regions physically becomes unstable: an unsteady boundary-layer model has to be used, whose validity, in turn, terminates with a Van Dommelen-Shen singularity [15]. In a consistent way, numerical simulation methods based on the thin boundary-layer concept tend to break down when the thickness of the separated-flow region becomes significant, e.g. [27, 87], thus giving a warning that the selected flow modelling should be reconsidered. Readers might wish to consult Chapter 14 of the enlarged edition of Schlichting's 'Boundary-Layer Theory' [60] for a more detailed discussion of these asymptotic issues.

4. Non-asymptotic points of view

In the late seventies, the quest for the cause of the singularity has also moved along non-asymptotic lines that in retrospect can be related to the above. Several investigations into the boundary-layer relation between pressure and displacement thickness have been carried out, which all produced a similar outcome.

First, we will present the reflections of LeBalleur [39] at ONERA. He considered an integral formulation of the turbulent boundary-layer equations, consisting of Von Kármán's integral equation and Head's entrainment equation. In case u_e is prescribed, these differential equations

are conveniently ordered as

$$\text{Von Kármán:} \quad \frac{\mathrm{d}\theta}{\mathrm{d}x} = \tfrac{1}{2}c_f - \frac{\theta}{u_e}(2 + H)\frac{\mathrm{d}u_e}{\mathrm{d}x} \,,$$

$$\text{Entrainment:} \quad H_1\frac{\mathrm{d}\theta}{\mathrm{d}x} + \theta\frac{\mathrm{d}H_1}{\mathrm{d}x} = \frac{E}{u_e} - \frac{\theta H_1}{u_e}\frac{\mathrm{d}u_e}{\mathrm{d}x} \,.$$

(9)

Here, θ is the momentum thickness, H the shape factor θ/δ^*, c_f the shear-stress coefficient, E Head's entrainment function and H_1 the entrainment shape factor (which is assumed to be a function of H only). The two differential equations are supplemented with three algebraic relations for determining H, E and c_f.
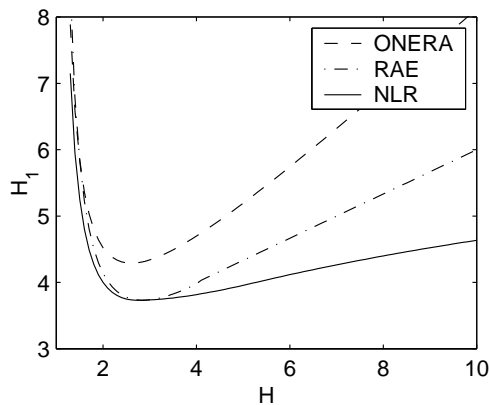

Figure 5: Some H-H_1 relationships as used at ONERA [39], RAE [44] and NLR [31] around 1980. The three relations agree on having a minimum near $H \approx 2.7$, corresponding with the onset of separation. For larger values of H the curves disagree, but experimental data to support these curves was rare at that time.

LeBalleur [39] demonstrated that the numerical problems at separation are caused by the algebraic relation between H and H_1. Since H_1 follows from the two differential equations (9), the algebraic relation should provide H. However the graph of H_1 as a function of H shows a minimum at (or nearby) a point of flow separation. Figure 5 gives versions of this relation as used at ONERA [39], RAE [44] and NLR [31] around that time; supporting experimental data can be found in the review paper by Lock and Williams [45]. As a consequence, not for every value of H_1 is it possible to find a value for H! LeBalleur further showed that when also u_e is considered as an unknown no difficulties arise (an extra equation has to be added that describes the interaction between inviscid flow and boundary layer).

As another example, a numerical experiment performed at the National Aerospace Laboratory NLR in Amsterdam will be described [77, 79]. In this study the original boundary-layer equations (1), i.e. as a field method, were solved with a prescribed displacement thickness chosen such that flow separation occurred. Then at a fixed x-station δ^* was varied, keeping every other station fixed, and the variations of u_e and the shear-stress coefficient c_f were studied. It turned out that in this way u_e as a function of δ^* possessed a minimum, that seemed to correspond (within one or two grid cells) with the point where c_f vanishes, i.e. a point of flow separation; Fig. 6 (left) gives the idea,[2] very resemblant of Fig. 5.

All similar studies [2, 30] suggested that the velocity distribution u_e cannot be prescribed arbitrarily near a point of flow separation. There is a certain range in u_e-values outside which no solution seems to exist, a situation correctly predicted by Goldstein some thirty years earlier.

---

[2]The curves have been copied from my research notes of 15 December 1977, drawn in pencil on millimeter paper. The scaling of the axes was not indicated, but it is not relevant: the locations of the minimum in u_e and of the zero of c_f are all that matter.
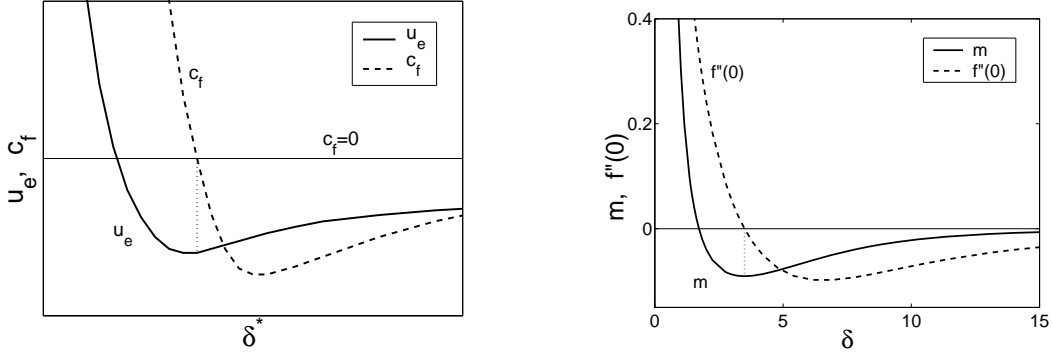
Figure 6: Behaviour of u_e and c_f as a function of δ^* at a fixed boundary-layer station *(left)*, and Falkner–Skan relation between pressure parameter m, shear stress $f''(0)$ and displacement parameter δ *(right)*. The left-hand graph is from boundary-layer calculations in 1977; the right-hand graph could have been drawn in 1954.

In terms of dynamical systems, passing the separation point with u_e prescribed amounts to crossing a saddle point [34, 37]. Another option has been to solve the boundary-layer equations with prescribed wall shear [35], but as will be obvious from Fig. 6 this option runs into similar diffculties. It would be interesting to study this issue from a theoretical point of view. Only little theory on existence and uniqueness of solutions of the boundary-layer equations exists [53, 54, 84], but with the current numerical evidence it is known what to look for.

In retrospect, it is not difficult to recognize that already earlier similar types of graphs could have been presented, e.g. in relation with the family of Falkner–Skan similarity solutions of the boundary-layer equations [20]. This family is governed by the equation

$$f''' + ff'' + \frac{2m}{m+1}(1 - f'^2) = 0 \,, \quad f(0) = f'(0) = 0 \,, \quad f'(\infty) = 1 \,,$$

where m is a parameter related to the pressure gradient through $m = x(\mathrm{d}u_e/\mathrm{d}x)/u_e$. In particular, the main branch of attached flow solutions only exists for $m > -0.0904$, whereas for $-0.0904 < m < 0$ also a separated flow branch exists; this branch was identified by Stewartson in 1954 [67]. Figure 6 *(right)* gives an unusual presentation of the Falkner–Skan results: the pressure parameter m and the shear variable $f''(0)$ are shown as a function of the displacement thickness δ (defined through $f(\eta) \sim \eta - \delta$ for $\eta \to \infty$); the resemblance with the much more recent graph in Fig. 6 *(left)* is striking!

5. Viscous-inviscid interaction methods

The above, mainly theoretical, considerations brought the insight to tackle engineering boundary-layer problems in an industrial context. The message is threefold:
– firstly, the boundary-layer approximation is sufficiently accurate to model the flow in mildly separated flow regions;
– secondly, the interaction involves and requires a local region of invisicd flow;[3]
– thirdly, and most important, the hierarchy between boundary layer and inviscid flow is lost.
Although for turbulent flow a different asymptotic structure exists [47], the messages from laminar-flow theory carry over, and in the discussion of Goldstein's singularity the distinction between laminar flow and turbulent flow is not relevant. It is good to realize that Goldstein's singularity has no fundamental physical basis, but it is created artificially by mathematically splitting the flow field in two hierarchical parts: a splitting against which the physics protests!

---

[3]Because of the second message, it makes no sense to apply the full Navier–Stokes equations in the boundary layer. 'Goldstein' will still strike back, unless the computational region is much thicker than the boundary layer.

Thus interactive boundary-layer models were proposed, where Prandtl's boundary-layer equations were coupled with a relation like (8), describing the main interaction with the inviscid flow, or with an accurate inviscid-flow solver. Such a coupled problem can be written as, in principle, two equations with two unknowns:

$$\text{external inviscid flow} \qquad u_e = E\left[\delta^*\right], \tag{10}$$

$$\text{boundary-layer flow} \qquad u_e = B\left[\delta^*\right]. \tag{11}$$

Here E denotes the external inviscid-flow operator, whereas B is the boundary-layer operator for prescribed displacement thickness; note that near flow separation the inverse B^{-1} does not exist. In the classical, or 'direct', method u_e is computed from the inviscid-flow equation in (10), whereas the displacement thickness is determined from the viscous flow equation in (11) with a breakdown of B^{-1} in separation.

Inspired by the theoretical developments described above, in the second half of the seventies a number of ideas have been brought forward to circumvent the breakdown singularity. The simplest way is to invert the direction of the iterative process in the classical method. One obtains the so-called 'inverse' method, where, following the idea set forward by Catherall and Mangler [6], the boundary layer is solved with prescribed displacement thickness. An early success was obtained by Carter [5] when he computed the separated flow past an indented plate. For engineering applications, however, the inverse method converges very slow, and it has not been used on large scale. To speed up convergence, other methods were developed, of which two have survived [45]: the semi-inverse method of LeBalleur [39, 40] and Carter [4], and the quasi-simultaneous method [76, 78].

Semi-inverse

The semi-inverse method (Fig. 7, left) introduced by LeBalleur in France [39, 40], and independently by Carter in the USA [4], is a mixture of the direct and the inverse method. It solves the boundary-layer equations with prescribed displacement thickness, and the inviscid flow in the traditional way (hence also with prescribed displacement thickness):

$$u_e^E = E\left[\delta^{*(n-1)}\right] \ \ (\text{direct}); \qquad u_e^B = B\left[\delta^{*(n-1)}\right] \ \ (\text{inverse});$$

$$\delta^{*(n)} = \delta^{*(n-1)} + \omega\left(u_e^B - u_e^E\right).$$

Experience in tuning the relaxation parameter ω has developed throughout the years, and many applications of the semi-inverse method, including massively separated flow(!), can be found in the literature, e.g. [21, 41, 55].
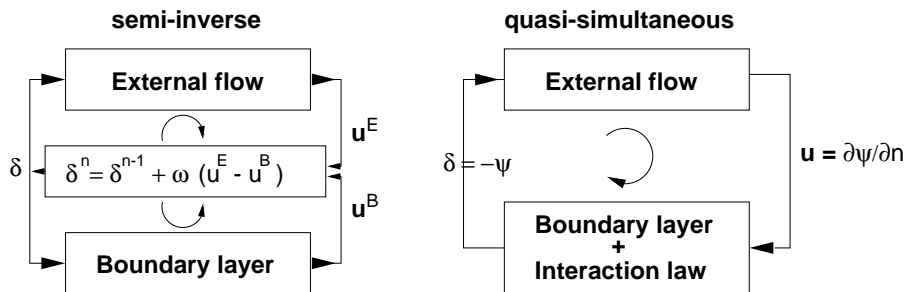

Figure 7: Semi-inverse and quasi-simultaneous VII method.

Quasi-simultaneous

The quasi-simultaneous method follows the suggestion made by Lagerstrom [38]. It wants to reflect the lack of hierarchy between both subdomains: in principle, it wants to solve both subdomain problems simultaneously. When the boundary layer is modelled by an integral formulation a simultaneous coupling is well feasible, with early examples dating back to the seventies already, e.g. [16, 22, 31, 50]. In principle, such a fully simultaneous approach is to be preferred. However, when in both domains a field formulation is chosen, software complexity may prohibit a practical implementation. Recall that around 1980 mainframe computers possessed a memory of only 1(!) Mbyte. At that time this prevented a fully simultaneous approach, and the idea was born to solve the boundary-layer equations simultaneously with a *simple* but good *approximation* of the inviscid flow, which was termed the interaction law. The difference between this approximation and the 'exact' inviscid flow can then be handled iteratively. In this way, the quasi-simultaneous method (Fig. 7, *right*) can be formulated as

$$
\begin{aligned}
u_e^{(n)} - I\left[\delta^{*(n)}\right] &= E\left[\delta^{*(n-1)}\right] - I\left[\delta^{*(n-1)}\right] , \\
u_e^{(n)} - B\left[\delta^{*(n)}\right] &= 0 ,
\end{aligned}
\tag{12}
$$

where (n) is the iteration count. Note that the VII iterations 'only' need to account for the difference between the external flow E and its approximation I. In other words, the interaction law is used in defect formulation: it does not influence the final converged result, but it circumvents Goldstein's singularity and enhances the VII convergence.

Next, the question arises how to choose the interaction law. A fair description of how an inviscid flow reacts on displacement effects is delivered by thin-airfoil theory, in its simplest form given by

$$
u_e(x) = u_{e0}(x) + I\left[\delta^*\right], \quad \text{with} \quad I\left[\delta^*\right] = \frac{1}{\pi} \int_\Gamma \frac{\mathrm{d}\delta^*}{\mathrm{d}\xi} \frac{\mathrm{d}\xi}{x - \xi} ,
\tag{13}
$$

where u_{e0} is the edge velocity without displacement effects. Also triple-deck theory provides this type of approximation, cf. (8), which makes the Cauchy–Hilbert integral in (13) a good candidate for an interaction law. Indeed, it has turned out to be successful. An example of the use of this interaction law (describing thickness effects) together with its skew-symmetric counterpart (describing camber effects) is given in Section 6.. Many other examples of the use of (13) can be found in the literature, for example in the monograph [7].

Later, when larger computers became available, in engineering applications this 'simple' interaction law has sometimes been replaced by more sophisticated ones, for instance interaction laws based on a discrete Laplace description of the inviscid flow [3], or based on an inviscid panel method (e.g. [11]). In this way a better convergence of the iterations in (12) can be obtained.

On the other hand, at least from a scientific point of view, it is interesting to find out how far the above interaction law can be simplified without being struck by Goldstein's singularity, while at the same time yielding acceptable convergence of the iterations in (12). We will pursue this question in Section 7..

Remark 4 In three dimensions a similar approach is feasible, with two thin-airfoil expressions like (13) relating the two inviscid surface-velocity components to the shape of the displacement body, as demonstrated for example by Roget *et al.* [58] and Edwards [18]. The latter author was largely inspired by Davis, who at the east coast of the USA has initiated research in interactive boundary layers [86]. Related work in the UK has been carried out by Smith and co-workers [63]. At the USA west coast Cebeci has been an active advocate of quasi-simultaneous VII methods in engineering applications (airfoil analysis and design) [10]. For three-dimensional engineering flow simulations much pioneering work has been done by Cousteix and his colleagues in France [8, 13, 58].

Remark 5 The interacting boundary-layer (IBL) formulation can be obtained from other considerations, such as the approach by Cousteix and Mauss [14] where the flow modelling is chosen according to the successive complementary expansion method. But, unavoidably, the threefold message presented at the beginning of this section has to be acknowledged. Other appearances of IBL methods can be found for example in [66].

6. Application to transonic airfoil flow

The performance of the quasi-simultaneous coupling concept will be demonstrated on a typical calculation of transonic flow past an RAE2822 airfoil with the NLR Vistrafs code. The boundary layer was modelled by Prandtl's equations with the algebraic Cebeci-Smith turbulence model; effects of streamline curvature were included [80]. The inviscid flow was modelled by transonic full potential theory. As an interaction law, the integral (13) has been used to describe the symmetric displacement effects ('thickness problem'), together with its skew-symmetric counterpart to describe the effects of camber ('lift problem'); for details see Veldman *et al.* [81].
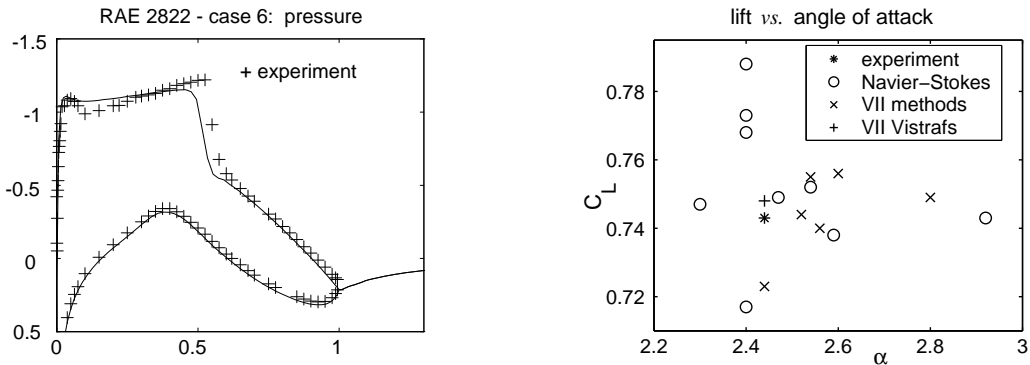

Figure 8: RAE2822 airfoil at M=0·725, Re=6·5mill., α=2·44, C_L=0·743 (Case 6). Pressure distribution *(left)* and comparison of lift predictions by various VII and NS methods [28] *(right)*.

The flow case presented in Fig. 8 is mildly transonic, with a small amount of separated flow near the trailing edge. Pertinent flow parameters are $M = 0·725$, Re = 6·5 million, $\alpha_{\exp} = 2·92$ (with a corrected value of $\alpha = 2·44$) and fixed transition at 3% chord.

The computational grid consists of 173×21 grid points (C-type, with 128 points along the airfoil surface) in the boundary layer, and the inviscid-flow grid was 128×64 (O-type). The computations require about 10 quasi-simultaneous iterations to converge to 3–4 digits, which on a modern PC takes less than one minute (it was so much different in the mid-eighties when this method was developed...). The rate of convergence is governed by the difference between the exact inviscid flow E and its approximation I; as a consequence it is independent of the grid size. To appreciate the fast convergence even better, one should realize that the external flow in this example is transonic, with a significant supersonic flow region, whereas the interaction law (13) is based on sub(!)sonic theory.

In 1986 this flow case has been the subject of a workshop [28], where about twenty aerodynamic codes were compared. The lift coefficient predicted by these codes is presented in Fig. 8 *(right)*, where a distinction has been made between viscous-inviscid interaction (VII) codes and Navier–Stokes codes. A similar situation was found for the other flow cases investigated in the workshop. The participants were also requested to quantify the computational complexity of their codes: it was found that, depending on the inviscid flow model used, VII codes were one to two orders of magnitude cheaper than Navier–Stokes codes. The latter codes required 10^6–10^7 floating-point operations per grid point; a price tag that is still representative for today's Navier–Stokes codes, as can be inferred from the review data presented by Agarwal [1].

A conclusion of the workshop must be that, in spite of their much smaller complexity, the quality of the VII results is comparable to that of the Navier–Stokes results. In fact, the quality of flow simulations for this type of flow appears to be dominated by the quality of the turbulence model. Any difference between a full Navier–Stokes model and a simplified boundary-layer model just drowns in the uncertainty in turbulence modelling. As stated by Holst [28]: *"An engineering turbulence model that can approximately predict the size and extent of separated regions is desperately needed."* Since 1986 the situation has not changed significantly. A European CFD validation project in 1992 once again revealed that the uncertainty due to turbulence modelling produces a large spreading of the Navier–Stokes results [25].

Of course, Navier–Stokes modelling is required in situations where the viscous region can no longer be considered as thin, such as massive flow separation in take-off and landing configurations, or the flow near essentially three-dimensional objects. In this respect it is remarkable that maximum-lift prediction with a VII method appears to be feasible, as demonstrated by Cebeci and co-workers [9, 10]; see also Section 9..

7. In search of a simpler interaction law

The implementation of an interaction law, be it the thin-airfoil expressions for thickness and camber or an influence matrix of a panel method, can be cumbersome. Therefore, it is worthwhile to investigate how much the interaction law can be simplified without being struck by Goldstein's singularity. The viscous-inviscid convergence is likely to deteriorate, but the effort to adapt an existing 'classical' boundary-layer code to separated-flow computations will be smaller. Thus, referring to the quasi-simultaneous formulation (12), the question is

How 'small' can I be chosen?

This question has been thoroughly investigated in the PhD thesis of Coenen [12]. She has performed an analysis based on the theory for non-negative matrices and the closely related M-matrices (see [29, 75]). We will first summarize the theory as developed by Coenen; thereafter the usefulness of the theory will be demonstrated on some realistic flow problems. As a reminder, it is remarked that $I = 0$ corresponds with the direct method that blows up in Goldstein's singularity.

A model problem

To shape the theory, as a model problem the flow past an indented plate (Fig. 9) is studied for which the external flow will be described by the thin-airfoil expression (13). It is our aim to construct a simple interaction law for this case. Let us first collect some properties of the operators E and B.
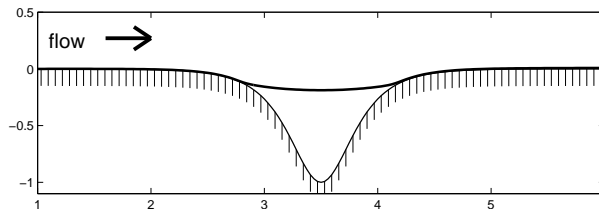
Figure 9: Geometry sketch of indented plate geometry.

External flow The integral (13) is discretized on a uniform grid with mesh size h. The displacement thickness δ^* is interpolated by a piece-wise linear function; only on the two intervals

13

adjacent to the Cauchy principal value a quadratic interpolation is used:

$$E\left[\delta^*\right] \equiv \frac{1}{\pi} \int_\Gamma \frac{\mathrm{d}\delta^*}{\mathrm{d}\xi} \frac{\mathrm{d}\xi}{x_i - \xi} = \frac{1}{\pi} \left\{ \int_{x_{i-1}}^{x_{i+1}} + \Sigma_{j \neq i-1,i} \frac{1}{\pi} \int_{x_j}^{x_{j+1}} \right\} \frac{\mathrm{d}\delta^*}{\mathrm{d}\xi} \frac{\mathrm{d}\xi}{x_i - \xi}$$

$$\approx -\frac{2h}{\pi} \left.\frac{\mathrm{d}^2\delta^*}{\mathrm{d}\xi^2}\right|_i + \frac{h}{\pi} \Sigma_{j \neq i-1,i} \left.\frac{\mathrm{d}\delta^*}{\mathrm{d}\xi}\right|_{j+1/2} \ln\left|\frac{i-j}{i-j-1}\right| . \quad (14)$$

After discretization of the ξ-derivatives in (14), the corresponding discrete matrix $\mathbf{E}$ is symmetric, positive definite with diagonal $4/\pi h$, and with non-positive off-diagonal entries.

Boundary-layer flow   Referring e.g. to [79], a discrete boundary-layer operator $\mathbf{B}$ typically is lower diagonal, with negative diagonal entries for attached flow and (slightly) positive diagonal entries for reversed flow; compare the slope of the (δ^*, u_e)-relation in Fig. 6 *(left)*.

8.   Matrix theory of viscous-inviscid interaction

To develop the theory, first the quasi-simultaneous method (12) will be rewritten in matrix notation

$$\left. \begin{array}{rcl} u_e^{(n)} - \mathbf{I}\,\delta^{*\,(n)} & = & (\mathbf{E} - \mathbf{I})\,\delta^{*\,(n-1)} \\ u_e^{(n)} - \mathbf{B}\,\delta^{*\,(n)} & = & 0 \end{array} \right\} \Rightarrow (\mathbf{I} - \mathbf{B})\,\delta^{*\,(n)} = (\mathbf{I} - \mathbf{E})\,\delta^{*\,(n-1)} . \quad (15)$$

After convergence, the ultimate system to be solved reads in matrix notation

$$(\mathbf{E} - \mathbf{B})\,\delta^* = 0 . \quad (16)$$

In this study we will consider situations with steady flow, for which it is natural to make the following assumption; moreover it allows theory to be developed:

> *Assumption*   The matrix $\mathbf{E} - \mathbf{B}$ is assumed to be (positive) stable, i.e. all its eigenvalues lie in the stable half plane, with positive diagonal entries and non-positive off-diagonal entries (hence it is an M-matrix).

VII iterations   An interaction law as in (15) corresponds with a splitting $\mathbf{E} - \mathbf{B} = (\mathbf{I} - \mathbf{B}) - (\mathbf{I} - \mathbf{E})$. When $\mathbf{I} \geq \mathbf{E}$, under the above assumption $\mathbf{I} - \mathbf{B}$ is an M-matrix, making $(\mathbf{I} - \mathbf{B})^{-1} \geq 0$ [29, p. 114]; hence this splitting is regular [75, p. 88]. As the off-diagonals of $\mathbf{E}$ are non-positive, this suggests to construct $\mathbf{I}$ from $\mathbf{E}$ by dropping one or more off-diagonals (Fig. 10). Since also $\mathbf{E} - \mathbf{B}$ is an M-matrix, the comparison theorem on regular splittings [75, p. 90] implies that the convergence of the VII iterations deteriorates monotonously with the number of dropped off-diagonals in $\mathbf{I}$.
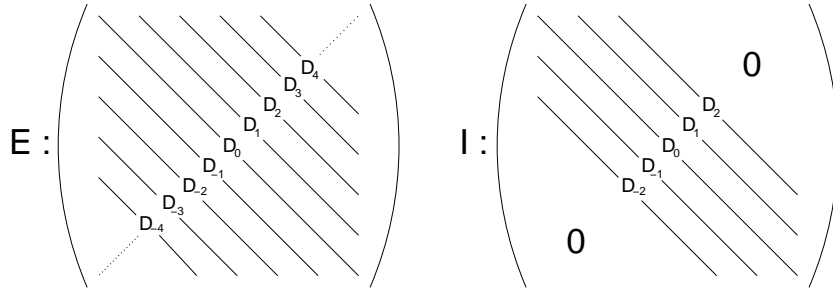

Figure 10: Tne interaction law $\mathbf{I}$ *(right)* may be obtained from the external flow matrix $\mathbf{E}$ *(left)* by omitting some off-diagonals (here only two diagonals on each side have been retained).

Boundary-layer iterations Each VII iteration a boundary-layer computation has to be performed, in which (15) is to be solved. This is done by repeated marching through the boundary layer, starting near the stagnation point and proceeding in downstream direction. Thus, a Gauss–Seidel type of iteration is performed. This method 'only' has to iterate on the upper triangular part of the matrix $\mathbf{I} - \mathbf{B}$, which here consists of entries from $\mathbf{I}$. Hence it may be expected that a 'small' upper-diagonal part will speed up convergence. And, indeed, under the above assumption it can be proven that the Gauss-Seidel convergence improves monotonously with the number of dropped off-diagonals in $\mathbf{I}$ [12]. This is opposite to the behaviour of the VII iterations, hence a trade-off is opportune (see below). Further, it is remarked that an interaction law which only consists of a main diagonal does not require boundary-layer iterations.
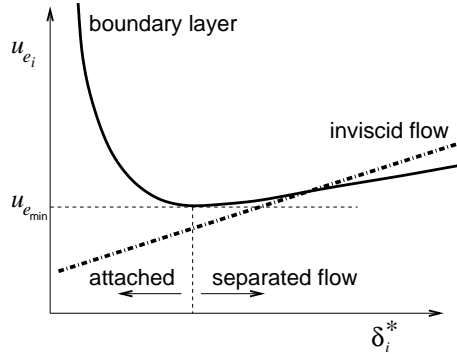

Figure 11: A sketch of the boundary-layer behaviour, combined with an inviscid-flow relation.

Robustness As already discussed in Section 4., the boundary-layer formulation is highly nonlinear. In Fig. 11 we copy Fig. 6 *(left)*, where, at a fixed boundary-layer station, the dependence between the edge velocity u_e and the displacement thickness δ^* is shown [79]. This sketch shows clearly that below a certain value of u_e no solution can be found anymore. Prescribing a linear combination of u_e and δ^*, as is the case when an interaction law is applied, should be useful provided the coefficient of δ^* stays sufficiently away from zero. Also during the iterations the process should not break down, hence the eigenvalues of the interaction matrix $\mathbf{I}$, and herewith the eigenvalues of $\mathbf{I} - \mathbf{B}$, should stay sufficiently far from the imaginary axis.

Again theory can be developed. With the above assumption, $\mathbf{I} - \mathbf{B}$ can be written as a constant positive diagonal matrix minus a non-negative matrix. For the latter type of matrices the largest eigenvalue grows monotonously with the matrix entries (the Perron-Frobenius theorem [75, p. 30]). Thus for $\mathbf{I} - \mathbf{B}$ this dependency holds for the smallest eigenvalue. With $\mathbf{I} \geq \mathbf{E}$, this eigenvalue is located in the stable half plane. Further, it grows with the number of dropped off-diagonals, herewith increasing the robustness of the boundary-layer calculation. Also in this respect an interaction law consisting of only the main diagonal of $\mathbf{E}$ scores best.

9. Simplified interaction in practice

Indented plate

The theory behind simplifying the interaction law will first be tested with the above indented plate (Fig. 9). The dent is about one unit wide and chosen quite deep in comparison with the boundary-layer thickness, which makes it a severe testcase for the VII algorithm. The Reynolds number based on unit length is 10^8. The boundary layer is modelled with Head's entrainment method [12].

The interaction law $\mathbf{I}$ is chosen by simply dropping off-diagonals in the 'exact' inviscid flow matrix $\mathbf{E}$. Figure 12 *(left)* gives the number of VII iterations as a function of the number of retained off-diagonals. Three flow situations have been distinguished: one with attached flow
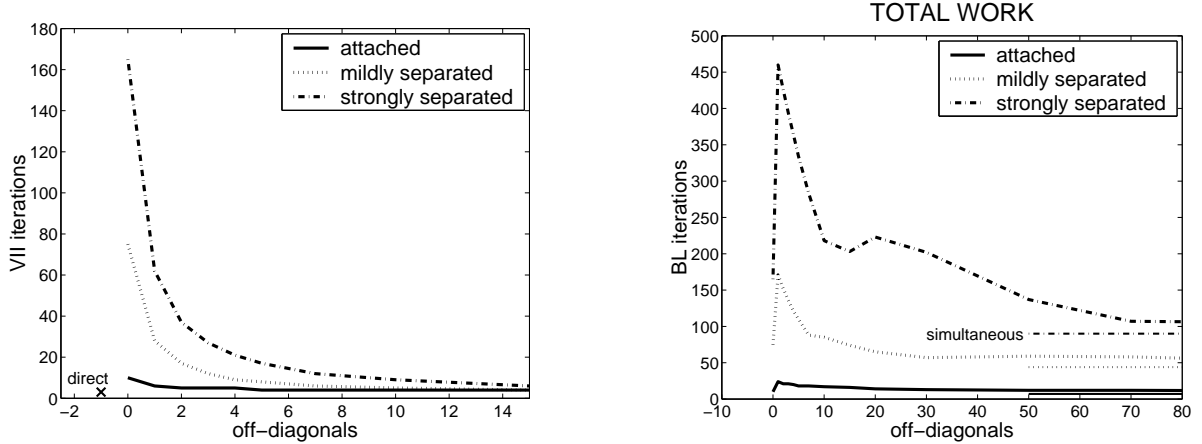
Figure 12: Number of VII iterations (*left*) and total number of boundary-layer sweeps (*right*) as a function of the number of retained off-diagonals.

(when the dent is very shallow), one with mild separation, and one with severe separation (as in Fig. 9).

For all choices of **I** the VII iterations are found to converge. Moreover, according to theory, the convergence of the VII iterations improves monotonously with the number of diagonals retained in **I**. The limit number of iterations is 2-3. For attached flow this can be compared with the direct method which also requires 3 iterations to converge (in the separated-flow cases the direct method breaks down).

Further, the number of VII iterations drops fast when the number of retained off-diagonals increases. On the other hand this leads to slower convergence of the boundary-layer iterations, and therefore the total number of boundary-layer sweeps has also been monitored in Fig. 12 *(right)*. A local minimum exists when the interaction law only consists of the main diagonal (in this case one boundary-layer sweep per VII iteration suffices). When one off-diagonal is added, the number of Gauss–Seidel sweeps per VII iteration increases, and herewith the total number of boundary-layer sweeps. Adding more off-diagonals the decrease in VII iterations becomes dominant. A minimum number of boundary-layer sweeps is found in the limit **I** → **E**. Here, the number of boundary-layer sweeps should be equal to the number required for a fully simultaneous treatment, i.e. when (16) is solved by Gauss–Seidel. Indeed, this is the case.

Thus for the interaction law two interesting choices exist. One option is to choose it according to the 'full' external flow; the other option is to choose it equal to only the diagonal $4/\pi h$ of the external-flow matrix. As the first option is against our quest for simplicity, below we will test the second option on a realistic problem of boundary-layer flow past a two-dimensional airfoil.

Subsonic airfoil flow

The above ideas on simplifying the interaction law will now be tested for aerodynamic flow past a NACA0012 airfoil (at $Re = 9 \cdot 10^6$, and $M_\infty = 0$); experimental data is available. The inviscid flow is modelled by potential theory, and computed by means of a panel method. Boundary layer plus wake are modelled with Head's entrainment method (for more information we refer to [12]). They are solved together with the interaction law

$$\mathbf{I} = \text{diag}\{4/\pi h\} \ . \tag{17}$$

We stress that this interaction law is unaware of the Kutta condition and its effect on the global circulation; it only accounts for the local VII physics – but this turns out to be sufficient!

A large part of the lift polar has been computed. The calculations turn out to be highly robust. It appears that even for separated-flow cases beyond maximum lift the calculations
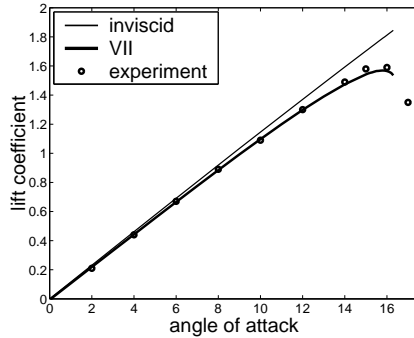
Figure 13: Lift polar for NACA0012 airfoil: viscous-inviscid calculation versus experiment.

converge without any need for a good initial guess; they can be started from scratch! The number of VII iterations with the extremely simple interaction law (17) typically is less than 100 at zero lift upto 1000 around maximum lift; only for larger angles of attack the computations break down. The number of iterations may sound large, but they can easily can be combined with the time-stepping in an unsteady inviscid-flow solver. Anyway, for two-dimensional simulations, the computing times count in just seconds on an average PC.

Remark 6 Experience with the above simplified interaction laws for three-dimensional boundary layers has been described in Coenen's PhD thesis [12].

10. Epilogue

Prandtl's 1904 boundary-layer theory formed the starting point for the viscous-inviscid interaction methods that have been developed in the last two decades of the 20th century. They have become very popular, since in comparison with brute-force Navier–Stokes solutions they are about two orders less expensive, whereas for flow conditions with thin shear layers the results are equally useful. Because of their modest computational complexity, they are ideal to be used in aerodynamic airfoil and wing optimization studies, e.g. [17, 65, 83, 85].

The greatest challenge has been to understand and resolve the singularity at separation, which occurs when the boundary-layer equations are solved with prescribed pressure. In 1948, Goldstein already foresaw the possibility that near separation in general no solution does exist, unless the pressure satisfies certain properties. Triple-deck theory provided the insight behind these difficulties, and gave the clue towards their solution. Goldstein turns out to have pointed in the right direction of non-existence; doubts on the validity of the boundary-layer model were found not to be essential here.

Stewartson and his 1969 contemporaries have provided the asymptotic framework valid near separation: the triple deck. In 1975 Lagerstrom described his view on the triple deck, and today we know that his paper contains the essential message required to overcome the singularity at a point of flow separation: boundary layer and inviscid flow have to be solved simultaneously. It is through this type of insight that the use of viscous-inviscid interaction methods in engineering applications could flourish.

An interesting question is how close one can get to Prandtl's original boundary-layer formulation of prescribed edge velocity without running into Goldstein's singularity. It was found that a simple modification suffices

$$\left(u_e + \frac{4}{\pi h} \delta^* \right)^{(\text{new})} = \left(u_e + \frac{4}{\pi h} \delta^* \right)^{(\text{old})} .$$

This slight change, unlikely to be further simplified, results in a highly robust calculation method, applicable to airfoil calculations beyond maximum lift.

17

Only a small, strongly personally biased, glimpse of the world-wide efforts in solving Prandtl's boundary-layer equations as challenged by Goldstein's separated-flow singularity could be discussed: emphasis has been on steady incompressible flow, whereas supersonic inviscid flow and unsteady flow separation have been scratched only superficially.[4] Many places in the literature can be found that, in retrospect, were close to unraveling the correct 'interactive' view, but where lack of computational power prevented a further pursuit at that moment. It would be interesting to analyse all these 'close encounters', and I hope to find another occasion to dig deeper into this intriguing 20th-century story.

References

[1] R. Agarwal, "Computational fluid dynamics of whole-body aircraft," *Ann. Rev. Fluid Mech.*, **31**, 125–169 (1999).

[2] P. Ardonceau, Th. Alziary and D. Aymer, "Calcul de l'interaction onde de choc/couche limite aves décollement." In: *Computation of Viscous-Inviscid Interactions*, AGARD-CP-291, paper 28 (1980).

[3] F. Arnold and F. Thiele, "Laplace interaction law for the computation of viscous airfoil flow in low- and high-speed aerodynamics," *AIAA J.*, **31**, 2178–2185 (1994).

[4] J.E. Carter, "Viscous-inviscid interaction analysis of turbulent separated flow." AIAA paper 81–1241 (1981).

[5] J.E. Carter and S.F. Wornom, "Solutions for incompressible separated boundary layers including viscous-inviscid interaction." In: *Aerodynamic Analysis Requiring Advanced Computers*, NASA SP-347, pp. 125–150 (1975).

[6] D. Catherall and K.W. Mangler, "The integration of the two-dimensional laminar boundary-layer equations past the point of vanishing skin friction," *J. Fluid Mech.*, **26**, 163–182 (1966).

[7] T. Cebeci, *An Engineering Approach to the Calculation of Aerodynamic Flows*, Springer Verlag, Berlin (1999).

[8] T. Cebeci and J. Cousteix, *Modelling and Computation of Boundary-Layer Flows*, Springer Verlag, Berlin (1999).

[9] T. Cebeci, H. Hefazi, F. Roknaldin and L.W. Carr, "Predicting stall and post-stall behaviour of airfoils at low Mach numbers," *AIAA J.*, **33**, 595–602 (1995).

[10] K.C. Chang, N. Alemdaroglu, U, Mehta and T. Cebeci, "Further comparisons of interactive boundary-layer and thin-layer Navier-Stokes procedures," *J. Aircraft*, **25**, 897–903 (1988).

[11] E.G.M. Coenen, "Quasi-simultaneous coupling for wing and airfoil flow." In: C.-H. Lai, P.E. Bjorstad, M. Cross and O.B. Widlund (eds.), *Domain Decomposition Methods in Science and Engineering*, Domain Decomposition Press, Bergen, pp. 197–205 (1999).

[12] E.G.M. Coenen, *Viscous-Inviscid Interaction with the Quasi-Simultaneous Method for 2D and 3D Airfoil Flow*. PhD thesis, University of Groningen (2001); available at: www.ub.rug.nl/eldoc/dis/science/-e.g.m.coenen.

[13] J. Cousteix, "Three-dimensional and unsteady boundary-layer computations," *Ann. Rev. Fluid Mech.*, **18**, 173–196 (1986).

[14] J. Cousteix and J. Mauss, "Approximations of the Navier–Stokes equations for high Reynolds number flows past a solid wall," *J. Comp. Appl. Math.*, **166**, 101–122 (2004).

[15] L.L. van Dommelen and S.F. Shen, "The spontaneous generation of the singularity in a separating laminar boundary layer," *J. Comput. Phys.*, **38**, 125–140 (1980).

[16] M. Drela and M.B. Giles, "Viscous-inviscid analysis of transonic and low Reynolds number airfoils," *AIAA J.*, **25**, 1347–1355 (1987).

---

[4]Nothing at all has been said about all the interesting physical phenomena to be observed in boundary layers. For this aspect, the reader is strongly referred to the 'classical' boundary-layer treatise by Schlichting [60], or a recent review paper by Van Ingen [32].

[17] M. Drela and M.B. Giles, "ISES: a two-dimensional viscous aerodynamic design and analysis code." AIAA paper 87–1118 (1987).

[18] D.E. Edwards, "Analysis of three-dimensional separated flow using interacting boundary-layer theory." In: F.T. Smith and S.N. Brown (eds.), *Boundary-Layer Separation*, Springer Verlag, Berlin, pp. 163–178 (1987).

[19] J.W. Elliott and F.T. Smith, "Dynamic stall due to unsteady marginal separation," *J. Fluid Mech.*, **179**, 489–512 (1987).

[20] V.M. Falkner and S.W. Skan, "Solutions of the boundary layer equation," *Phil. Mag.*, **12**, 865–896 (1931).

[21] C.C. Fenno, P.A. Newman and H.A. Hassan, "Unsteady viscous-inviscid interaction procedures for transonic airfoils using Cartesian grids," *J. Aircraft*, **26**, 723–730 (1989).

[22] K. Fuji and K. Karashima, "A numerical approach to subsonic viscous-inviscid interaction," Report 575, Institute of Space and Aeronautical Science, University of Tokyo (1979).

[23] S. Goldstein, "On laminar boundary layer flow near a point of separation," *Quart. J. Mech. Appl. Math.*, **1**, 43–69 (1948).

[24] H. Görtler and W. Tollmien (eds.), *50 Jahre Grenzschichtforschung*, Vieweg Verlag, Braunschweig (1955).

[25] W. Haase, F. Brandsma, E. Elsholz, M. Leschziner and D. Schwamborn (eds.), *EUROVAL — An European Initiative on Validation of CFD Codes*, Notes on Numerical Fluid Mechanics 42, Vieweg Verlag, Braunschweig (1993).

[26] W.D. Hayes and R.F. Probstein, *Hypersonic Flow Theory*, Academic Press (1959).

[27] R.A.W.M. Henkes and A.E.P. Veldman, "On the breakdown of the steady and unsteady interacting boundary-layer description," *J. Fluid Mech.*, **179**, 513–529 (1987).

[28] T.L. Holst, "Viscous Transonic Airfoil Workshop - Compendium of Results," AIAA paper 87–1460 (1987).

[29] R.A. Horn and C.R. Johnson, *Topics in Matrix Analysis*, Cambridge University Press (1991).

[30] H.P. Horton, "Numerical investigation of regular laminar boundary layer separation." In: *Flow separation*, AGARD-CP-168, paper 7 (1975).

[31] R. Houwink and A.E.P. Veldman, "Steady and unsteady separated flow computation for transonic airfoils," AIAA paper 84–1618 (1984).

[32] J.L. van Ingen, "Looking back at forty years of teaching and research in Ludwig Prandtl's heritage of boundary layer flows." *Z. Angew. Math. Mech.*, **78**, 3–20 (1998).

[33] C.E. Jobe and O.R. Burggraf, "The numerical solution of the asymptotic equations of trailing edge flow," *Proc. Roy. Soc. London* A, **340**, 91–111 (1974).

[34] J.M. Klineberg and J.L. Steger, "Calculation of separated flows at subsonic and transonic speeds." In: H. Cabannes and R. Temam (eds.) *Proc. 3rd Int. Conf. Num. Meth. Fluid Mech*, Springer Verlag, Berlin, pp. 161–168 (1972).

[35] J.M. Klineberg and J.L. Steger, "On laminar boundary layer separation," AIAA paper 74–94 (1974).

[36] A. Kluwick, "Interacting boundary layers," *Z. Angew. Math. Mech.*, **67**, T3–13 (1987).

[37] A. Kumar and K.S. Yajnik, "Internal separated flows at large Reynolds number," *J. Fluid Mech.*, **97**, 27–51 (1980).

[38] P.A. Lagerstrom, "Solutions of the Navier–Stokes equation at large Reynolds number," *SIAM J. Appl. Math.*, **28**, 202–214 (1975).

[39] J.C. LeBalleur, "Couplage visqueux-non visqueux: analyse du problème incluant décollements et ondes de choc," *La Recherche Aérospatiale*, **1977-6**, 349–358 (1977).

[40] J.C. LeBalleur, "Couplage visqueux-non visqueux: méthode numérique et applications aux écoulements bidimensionnels transsoniques et supersoniques," *La Recherche Aérospatiale*, **183**, 65–76 (1978).

[41] J.C. LeBalleur, "New possibilities of viscous-inviscid numerical techniques for solving viscous flow equations with massive separation," In: T. Cebeci (ed.) *Numerical and Physical Aspects of Aerodynamic Flow IV*, Springer Verlag, Berlin, pp. 71–96 (1990).

[42] M.J. Lighthill, "On boundary layers and upstream influence I. A comparison between subsonic and supersonic flows," *Proc. Roy. Soc. London* A, **217**, 478–507 (1953).

[43] M.J. Lighthill, "On displacement thickness," *J. Fluid Mech.*, **4**, 383–392 (1958).

[44] R.C. Lock, "Prediction of the drag of wings at subsonic speeds by viscous-inviscid interaction techniques." In: AGARD-R-723, paper 10 (1985).

[45] R.C. Lock and B.R. Williams, "Viscous-inviscid interactions in external aerodynamics," *Prog. Aerospace Science*, **24**, 51–171 (1987).

[46] R.E. Melnik and R. Chow, *Asymptotic Theory of Twodimensional Trailing Edge Flows*. Grumman Research Department, Report RJ-510J (1975).

[47] R.E. Melnik, R. Chow and H.R. Mead, "Theory of viscous transonic flow over airfoils at high Reynolds number," AIAA paper 77-680 (1977).

[48] A.F. Messiter, "Boundary-layer flow near the trailing edge of a flat plate," *SIAM J. Appl. Math.*, **18**, 241–257 (1970).

[49] R.E. Meyer, "A view of the triple deck," *SIAM J. Appl. Math.*, **43**, 639–663 (1983).

[50] H.L. Moses, R.R. Jones III, W.F. O'Brien Jr. and R.P. Peterson, "Simultaneous solution of the boundary layer and freestream with separated flow," *AIAA J.*, **16**, 61–66 (1978).

[51] A.H. Nayfeh, "Triple-deck structure," *Comp. Fluids*, **20**, 269–292 (1991).

[52] V.Ya. Neiland, "Towards a theory of separation of the laminar boundary layer in a supersonic stream," *Mekh. Zhid. Gaza*, **4**, 53–57 (1969); English translation in *Fluid Dynamics*, **4**, 33–55 (1970).

[53] K. Nickel, "Prandtl's boundary-layer theory from the viewpoint of a mathematician," *Ann. Rev. Fluid Mech.*, **5**, 405–428 (1973).

[54] O.A. Oleinik and V.N. Samokhin, *Mathematical Models in Boundary Layer Theory*, Chapman and Hall (1999).

[55] C.R. Olling and G.S. Dulikravich, "Porous aerofoil analysis using viscous-inviscid coupling at transonic speeds," *Int. J. Num. Meth. Fluids*, **7**, 103–129 (1987).

[56] K. Oswatitsch and K. Wieghardt, "Ludwig Prandtl and his Kaiser-Wilhelm-Institut," *Ann. Rev. Fluid Mech.*, **19**, 1–25 (1987).

[57] L. Prandtl, "Ueber Fluessigkeitsbewegung mit kleiner Reibung." In: *Verhandlungen des dritten internationalen Mathematischen Kongresses, Heidelberg*, Teubner Verlag, Leipzig, pp. 484–491 (1905).

[58] C. Roget, J.Ph. Brazier, J. Cousteix and J. Mauss, "A contribution to the physical analysis of separated flows past three-dimensional humps," *Eur. J. Mech. B*, **17**, 307–329 (1998).

[59] A.P. Rothmayer and F.T. Smith, "Numerical solution of two-dimensional steady triple-deck problems." In: R.W. Johnson (ed.) *The Handbook of Fluid Dynamics*, CRC Press, Boca Raton, Chapter 25 (1998).

[60] H. Schlichting and K. Gersten, *Boundary-Layer Theory*, 8th revised and enlarged edition, Springer Verlag, Berlin (2000).

[61] F.T. Smith, "On the high-Reynolds number theory of laminar flows," *IMA J. Appl. Math.*, **28**, 207–281 (1982).

[62] F.T. Smith, "Steady and unsteady boundary-layer separation," *Ann. Rev. Fluid Mech.*, **18**, 197–220 (1986).

[63] F.T. Smith, "Steady and unsteady 3-d interactive boundary layers," *Comp. Fluids*, **20**, 243–268 (1991)

[64] F.T. Smith and J.H. Merkin, "Triple-deck solutions for subsonic flow past humps, steps, concave or convex corners and wedged trailing edges," *Comp. Fluids*, **10**, 7–25 (1992).

[65] P.D. Smith, "A viscous package for attached and separated flows on swept and tapered wings," RAE Technical Report 89027 (1989).

[66] I.J. Sobey, *Introduction to Interactive Boundary Layer Theory*, Oxford University Press (2000).

[67] K. Stewartson, "Further solutions of the Falkner-Skan equation," *Proc. Cambridge Phil. Soc.*, **50**, 454-465 (1954).

[68] K. Stewartson, "On the flow near the trailing edge of a flat plate II," *Mathematika*, **16**, 106–121 (1969).

[69] K. Stewartson, "Multi-structured boundary layers on flat plates and related bodies," *Advances in Applied Mechanics* **14**, 145–239 (1974).

[70] K. Stewartson, "D'Alembert's paradox," *SIAM Review*, **23**, 308–343 (1981).

[71] K. Stewartson, F.T. Smith and K. Kaups, "Marginal separation," *Stud. Appl. Math.*, **67**, 45–61 (1982).

[72] K. Stewartson and P.G. Williams, "Self-induced separation," *Proc. Roy. Soc. London* A, **312**, 181–206 (1969).

[73] V.V. Sychev, A.I. Ruban, V.V. Sychev and G.L. Korolev, *Asymptotic Theory of Separated Flows*. Cambridge: Cambridge University Press (1998).

[74] M. Van Dyke, "Nineteenth-century roots of the boundary-layer idea," *SIAM Review*, **36**, 415–424 (1994).

[75] R.S. Varga, *Matrix Iterative Analysis*, Prentice-Hall (1962).

[76] A.E.P. Veldman, "A numerical method for the calculation of laminar incompressible bounday layers with strong viscous-inviscid interaction." National Aerospace Laboratory, Report NLR TR 79023 (1979).

[77] A.E.P. Veldman, "Boundary layers with strong interaction: from asymptotic theory to calculation method." In: J.J.H. Miller (ed.), *Proc. BAIL 1 Conf. on Boundary and Interior layers*, Boole Press, Dublin, pp. 149–163 (1980).

[78] A.E.P. Veldman, "New, quasi-simultaneous method to calculate interacting boundary layers," *AIAA J.*, **19**, 79–85 (1981).

[79] A.E.P. Veldman, "A numerical view on strong viscous-inviscid interaction." In: W.G. Habashi (ed.) *Computational Methods in Viscous Flows*, Pineridge Press, Southampton, pp. 343–363 (1984).

[80] A.E.P. Veldman, "Matched asymptotic expansions and the numerical treatment of viscous-inviscid interaction," *J. Engng Math.*, **39**, 189–206 (2001).

[81] A.E.P. Veldman, J.P.F. Lindhout, E. de Boer, and M.A.M. Somers, "Vistrafs: a simulation method for strongly-interacting viscous transonic flow." In: T. Cebeci (ed.) *Numerical and Physical Aspects of Aerodynamic Flow IV*, Springer Verlag, Berlin, pp. 37–51 (1990).

[82] A.E.P. Veldman and A.I. van de Vooren, "Drag of a finite flat plate." In: R.D. Richtmayer (ed.) *Proc. 4th Int. Conf. Num. Meth. Fluid Dyn.*, Springer Verlag, Berlin, pp. 422–430 (1976).

[83] A. Verhoff, H.H. Chen, T. Cebeci and T. Michal, "An accurate and efficient interactive boundary-layer method for analysis and design of airfoils," AIAA paper 96–0328 (1996).

[84] W. Walter, "Existence and convergence theorems for the boundary layer equations based on the line method," *Arch. Rat. Mech. Anal.*, **39**, 169–188 (1970).

[85] A.J. van der Wees and J. van Muijden, "A fast and robust viscous-inviscid interaction solver for transonic flow about wing/body configurations on the basis of full potential theory," AIAA paper 93–3026 (1993).

[86] M.J. Werle, "R. Thomas Davis — His contributions to numerical simulation of viscous flows: Part II — Technical perspective," AIAA paper 88–0602 (1988).

[87] Z. Xiao, E.C. Adams and A.T. Conlisk, "Terminal structure of unsteady classical and interacting boundary layers," *Phys. Fluids,* **8**, 1397–1407 (1996).